Light Scattering by Spherical Particles: Radiation Pressure, Asymmetry Factor, and Extinction Cross Section

WILLIAM M. IRVINE
Harvard College Observatory and Smithsonian Astrophysical Observatory, Cambridge, Massachusetts 02138

(Received 14 August 1964)

The normalized cross sections for radiation pressure (Q_{pr}), extinction (Q_{ext}), and scattering (Q_{sca}) and the asymmetry factor $\langle\cos\theta\rangle$ were computed from the Mie scattering theory for size parameters in the range $0.5\leq x\leq 30$ and for $x\to\infty$ for both dielectric and absorbing particles. Additional values were obtained for $m=1.33$ and $50\leq x\leq 51$ and $100\leq x\leq 102$. The results are discussed and examples are presented in graphical form.

INTRODUCTION AND DEFINITIONS

THE scattering of a plane, monochromatic, electromagnetic wave by an homogeneous, isotropic sphere is described by Mie's solution[1] to Maxwell's equations. A number of computations using the Mie theory have appeared in the past few years. The Mie coefficients, the scattering and extinction cross sections, and the scattered intensity and polarization have all been described.[2–7] Two important quantities characteristic of the scattering have *not*, however, received much attention: the normalized cross section for radiation pressure Q_{pr} and the asymmetry factor $\langle\cos\theta\rangle$.

If unit irradiance is incident on a particle of cross-sectional area A, the force on the particle resulting from radiation pressure is

$$F=(A/c)Q_{pr}, \tag{1}$$

where c is the velocity of light. Equation (1) defines Q_{pr}.

The representation of the scattered intensity as a function of angle θ is known as the scattering diagram of the particle. When suitably normalized, the function shown by the scattering diagram is called the phase function $p(\theta)$. The mean over the sphere of the cosine of the scattering angle, weighted by the phase function, is called the asymmetry factor $\langle\cos\theta\rangle$. Thus,

$$\frac{1}{2}\int_{-1}^{1} d(\cos\theta)p(\theta)=1, \tag{2}$$

$$\frac{1}{2}\int_{-1}^{1} d(\cos\theta)\cos\theta p(\theta)=\langle\cos\theta\rangle. \tag{3}$$

The asymmetry factor is a useful parameter with which to characterize the relative importance of forward-to-backward scattering. It fits naturally into investigations of the scattering by interstellar particles,[8] into the theory of neutron diffusion,[9] and also into problems of multiple scattering by large particles.[10] The asymmetry factor has the additional virtue of being directly expressible in terms of the Mie coefficients, so that it may be evaluated without explicit knowledge of $p(\theta)$.

The quantities Q_{pr} and $\langle\cos\theta\rangle$ are related to the normalized scattering and extinction cross sections Q_{sca} and Q_{ext} by

$$Q_{pr}=Q_{ext}-\langle\cos\theta\rangle Q_{sca}. \tag{4}$$

In computations it is simplest to consider the three quantities on the right side of Eq. (4) as fundamental.

The basic theoretical discussion of radiation pressure on spheres, based on the Mie theory, was given by Debye.[11] The parameters of the theory are the particle size parameter $x=2\pi r/\lambda$, where r is the particle radius and λ is the wavelength of the radiation, and the complex index of refraction $m=\nu-i\nu'$. Except for a few isolated values[12] for small x, the previous calculations of $\langle\cos\theta\rangle$ (and hence Q_{pr}) have been confined to dielectrics and to perfect conductors ($m=\infty$). The results have been discussed by Irvine,[13] who also examined the limiting cases of Rayleigh–Gans scattering ($|m-1|\ll 1$ and $2x|m-1|\ll 1$) and of very large dielectric spheres ($x\gg 1$ and $2x(\nu-1)\gg 1$).

In the present paper we obtain more detailed results for Q_{pr} and $\langle\cos\theta\rangle$ for dielectrics and also extend the discussion to absorbing spheres. In addition, the behavior of Q_{ext} and Q_{sca} as a function of x, ν, and ν' is revealed in new detail. Specifically, if we define

$$\tan\beta=\nu'/(\nu-1), \tag{5}$$

the present discussion is based on calculations for the cases:

[1] G. Mie, Ann. Physik **25**, 377 (1908).
[2] D. Deirmendjian, R. Clasen, and W. Viezee, J. Opt. Soc. Am. **51**, 620 (1961).
[3] R. Penndorf, J. Opt. Soc. Am. **52**, 402 (1962).
[4] M. Kerker and E. Matijević, J. Opt. Soc. Am. **51**, 87 (1961).
[5] R. H. Giese, F. de Bary, K. Bullrich, and C. D. Vinnemann, Abhandl. Deut. Akad. Wiss. Berlin, Kl. Math. Phys. Tech. **6** (1961).
[6] B. M. Herman and L. J. Battan, Quart. J. Roy. Meteorol. Soc. **87**, 223 (1961).
[7] H. Walter, Optik **16**, 401 (1959).
[8] C. J. van Houten, Bull. Astron. Inst. Neth. **16**, 1 (1961).
[9] S. Glasstone and M. C. Edlund, *The Elements of Nuclear Reactor Theory* (D. Van Nostrand Company, Inc., Princeton, New Jersey, 1952), chap. 5.
[10] H. C. van de Hulst and W. M. Irvine, Mem. Soc. Roy. Sci. Liège **7**, 78 (1963).
[11] P. Debye, Ann. Physik **30**, 57 (1909).
[12] H. C. van de Hulst, *Light Scattering by Small Particles* (John Wiley & Sons, Inc., New York, 1950), Sec. 14.22; hereafter referred to as L. S.
[13] W. M. Irvine, Bull. Astron. Inst. Neth. **17**, 176 (1963). The value for $m=1.33$, $x=7.0$ in Table I of this paper should be 0.8350.

(1) $\nu=1.20$, 1.33, 1.50, ∞; $\tan\beta=0$, 0.01, 0.1, 1.0, 10; $0.5\leq x\leq 30$, with steps $\Delta x=0.1$, 0.05, or 0.025, depending on the complexity of the functions of x, with further intermediate values of $\tan\beta$ and x used when necessary to reveal the detail of the curves;

(2) $m=1.33$; $x=50(0.01)51$, $x=100(0.01)102$;

(3) $x\gg 1$; $2x|m-1|\gg 1$; $\tan\beta=0.0001$, 0.001, 0.01, 0.1, 1.0, 10.

PROCEDURE

Calculations from the Complete Mie Theory

The details of the Mie theory have been well described by van de Hulst (L.S.). We shall use his notation for the Mie coefficients a_n and b_n. Then the quantities of interest are

$$\langle\cos\theta\rangle=\frac{4}{x^2Q_{\rm sca}}\sum_{n=1}^{\infty}\left[\frac{n(n+2)}{(n+1)}\,{\rm Re}(a_na_{n+1}{}^*+b_nb_{n+1}{}^*)+\frac{2n+1}{n(n+1)}\,{\rm Re}(a_nb_n{}^*)\right], \quad (6)$$

$$Q_{\rm sca}=\frac{2}{x^2}\sum_{n=1}^{\infty}(2n+1)[|a_n|^2+|b_n|^2], \quad (7)$$

$$Q_{\rm ext}=\frac{2}{x^2}\sum_{n=1}^{\infty}(2n+1)\,{\rm Re}(a_n+b_n), \quad (8)$$

where the asterisk indicates complex conjugate (as has been pointed out previously,[13] the asterisks were accidentally omitted in L.S.). The quantity $Q_{\rm pr}$ is obtained from Eq. (4).

When the scattering particle is perfectly reflecting ($\nu=\infty$ or $\nu'=\infty$), van de Hulst's expressions for a_n and b_n simplify to

$$a_n=\psi_n'(x)/\zeta_n'(x),\qquad b_n=\psi_n(x)/\zeta_n(x). \quad (9)$$

The computational algorithm used to obtain a_n and b_n, and an analysis of the errors therein, is described elsewhere.[14] We mention here only that this computation, and hence the sums in Eqs. (6), (7), and (8), were broken off when $|a_n|^2+|b_n|^2<2(10)^{-12}$ and that the resulting values of $Q_{\rm sca}$, $\langle\cos\theta\rangle$, and $Q_{\rm ext}$ agreed with existing tabulations[13,15–17] to the full accuracy of the latter.

Very Large Spheres

Debye[11] has given an asymptotic form of the Mie equations valid when $x\gg 1$ and $2x|m-1|\gg 1$. An interpretation of the resulting formulas in terms of geometric optics has been made by van de Hulst.[18] If the particles are sufficiently absorbing that we need consider only reflected rays plus diffraction, the relevant expressions for incident unpolarized light are

$$Q_{\rm ext}=2, \quad (10)$$

$$Q_{\rm sca}=1+w, \quad (11)$$

$$\langle\cos\theta\rangle=(1+wg)/(1+w), \quad (12)$$

$$Q_{\rm pr}=1-wg, \quad (13)$$

where

$$w=\frac{1}{2}\int_0^1 d\sigma(|r_1|^2+|r_2|^2) \quad (14)$$

and

$$g=\frac{1}{2w}\int_0^1 d\sigma(2\sigma-1)(|r_1|^2+|r_2|^2) \quad (15)$$

are the contributions to $Q_{\rm sca}$ and $\langle\cos\theta\rangle$ resulting from reflected and refracted light only (i.e., treating the diffracted light as unscattered; see L. S. Sec. 12.5 and Ref. 10). In addition, the quantity $\sigma=\cos^2\tau$, r_1 and r_2 are the Fresnel reflectances:

$$r_1=\frac{\sin\tau-m\sin\tau'}{\sin\tau+m\sin\tau'},\qquad r_2=\frac{m\sin\tau-\sin\tau'}{m\sin\tau+\sin\tau'}; \quad (16)$$

the angle τ is the complement of the angle of incidence of a ray on the particle surface, and τ' is given by Snell's law: $m\cos\tau'=\cos\tau$. Since m and thus τ' are in general complex, formation of $|r_1|^2$ and $|r_2|^2$ is not trivial. Following the procedure of Born and Wolf,[19] we find

$$|r_1|^2=\frac{[(1-\sigma)^{\frac{1}{2}}-U]^2+V^2}{[(1-\sigma)^{\frac{1}{2}}+U]^2+V^2}; \quad (17)$$

$$|r_2|^2=\frac{[(\nu^2-\nu'^2)(1-\sigma)^{\frac{1}{2}}-U]^2+[2\nu\nu'(1-\sigma)^{\frac{1}{2}}+V]^2}{[(\nu^2-\nu'^2)(1-\sigma)^{\frac{1}{2}}+U]^2+[2\nu\nu'(1-\sigma)^{\frac{1}{2}}-V]^2}; \quad (18)$$

where

$$U=\left\{\frac{\nu^2-\nu'^2-\sigma+[(\nu^2-\nu'^2-\sigma)^2+4\nu^2\nu'^2]^{\frac{1}{2}}}{2}\right\}^{\frac{1}{2}},$$

and

$$V=-\left\{\frac{[(\nu^2-\nu'^2-\sigma)^2+4\nu^2\nu'^2]^{\frac{1}{2}}-(\nu^2-\nu'^2-\sigma)}{2}\right\}^{\frac{1}{2}}.$$

The expressions for w and g were evaluated using Simpson's rule and an interval in σ of 0.001. Variation

[14] W. M. Irvine, J. Cherniack, and J. Francis (to be published).

[15] R. H. Giese, Z. Astrophys. 51, 119 (1961). Unfortunately, the values of $Q_{\rm pr}$ tabulated by Giese were calculated from an incorrect formula [Ref. (13) and R. H. Giese, private communication, 1963].

[16] R. Penndorf, "New Tables of Mie Scattering Functions for Spherical Particles," Geophys. Research Paper No. 45, Part 6, 98 pp. (1956).

[17] W. J. Pangonis, W. Heller, and A. Jacobson, *Tables of Light Scattering Functions for Spherical Particles* (Wayne State University Press, Detroit, 1957).

[18] H. C. van de Hulst, Rech. Astron. Obs. d'Utrecht **XI**, Part 1, 87 pp. (1946).

[19] M. Born and E. Wolf, *Principles of Optics* (Pergamon Press, Inc. New York, 1959), Sec. 13.4.

of the interval and of the integration scheme assure that the results, which are presented in Table I, are

TABLE I. Radiation pressure and asymmetry factor for very large absorbing spheres (Sec. IIb).

m	$\tan\beta$	Q_{pr}	$\langle\cos\theta\rangle$	g	w
1.20	10^{-4}	0.97071	0.98563	0.6612	0.0443
	10^{-2}	0.97071	0.98562	0.6612	0.0443
	10^{-1}	0.97059	0.98551	0.6601	0.0445
	1	0.96228	0.97461	0.5825	0.0648
	10	0.97706	0.68775	0.0471	0.4874
1.33	10^{-4}	0.96415	0.97177	0.5436	0.0659
	10^{-2}	0.96415	0.97176	0.5436	0.0660
	10^{-1}	0.96403	0.97153	0.5423	0.0663
	1	0.95661	0.95086	0.4459	0.0973
	10	0.99904	0.59884	0.0014	0.6715
1.50	10^{-4}	0.96066	0.95196	0.4286	0.0918
	10^{-2}	0.96066	0.95196	0.4286	0.0918
	10^{-1}	0.96057	0.95158	0.4271	0.0923
	1	0.95575	0.91802	0.3218	0.1375
	10	1.00800	0.55289	−0.0101	0.7942
1.75	10^{-4}	0.96059	0.92209	0.3098	0.1272
	10^{-2}	0.96058	0.92208	0.3097	0.1272
	10^{-1}	0.96054	0.92149	0.3082	0.1280
	1	0.96015	0.87134	0.2060	0.1934
	10	1.00970	0.52796	−0.0111	0.8757

accurate to better than ± 0.00002 for Q_{pr} and $\langle\cos\theta\rangle$ and better than ± 0.0001 for g and w.

RESULTS FOR FINITE SIZE

Dielectrics

(1) Q_{ext}. The major oscillations (L.S., Sec. 11.22) corresponding to interference between diffracted and directly transmitted light are apparent in Figs. 1, 2, and 3.

The superimposed minor oscillations or "ripple" are illustrated more fully than by previous computations. The development of the ripple as x increases shows certain similarities for the three values of m considered. First, a single minor oscillation (the "first component" of the ripple) appears and increases in amplitude, apparently reaching a limiting value; the period of this first component seems to remain constant as x increases, but the maximum becomes confined to an increasingly

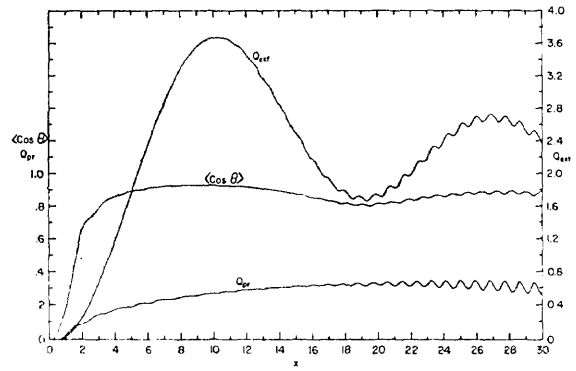

FIG. 1. Asymmetry factor $\langle\cos\theta\rangle$ and cross sections for extinction Q_{ext} and radiation pressure Q_{pr} for dielectric spheres with $m=1.20$. Computations made for $x=0.5(0.1)\ 10(0.05)\ 20(0.025)\ 30$.

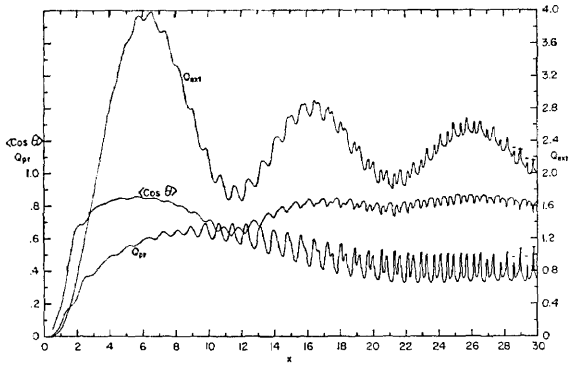

FIG. 2. Asymmetry factor $\langle\cos\theta\rangle$ and cross sections for extinction Q_{ext} and radiation pressure Q_{pr} for dielectric spheres with $m=1.33$. Computations made for $x=0.5(0.1)\ 10(0.05)\ 20(0.025)\ 30$. Horizontal dashes give height of resonance peaks determined from spot checks with $\Delta x=0.01$.

narrow resonance peak (Figs. 2 and 3). Meanwhile, a second minor oscillation (second ripple component) appears, at least for $m \gtrsim 1.33$, and undergoes the same development as the first component. Calculations for $m=1.33$ and $x=50(0.01)51$ and $x=100(0.01)102$ show only the two ripple components that are apparent for $17 \lesssim x \lesssim 30$ (Figs. 4 and 5). For $m=1.50$, the pattern is more complex. There appears to be at least one more component of the ripple, which tends to merge with the primary and secondary components. This process is hard to follow because of the extreme narrowness of these resonance peaks. These minor oscillations are neither strongly damped nor so irregular as would appear from Penndorf's[16] calculations, which utilized a Δx of 0.1. In order to detect the regularity of this fine structure, however, it is necessary to use an ever finer net of points as x and m increase. To investigate in detail a region such as $m=1.50$, $x>20$ (Fig. 3), would require a very small value of Δx indeed. Fortunately, this should not be necessary for physical applications.

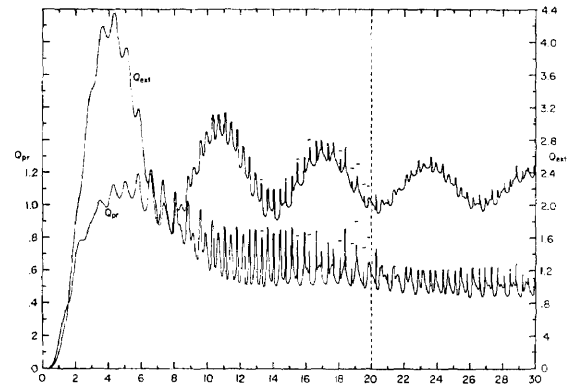

FIG. 3. Cross sections for extinction Q_{ext} and radiation pressure Q_{pr} for dielectric spheres with $m=1.50$. Computations made for $x=0.5(0.1)\ 10(0.05)\ 20(0.025)\ 30$. Horizontal dashes give height of resonance peaks determined from spot checks with $\Delta x=0.01$. Very narrow peaks are omitted for $x>20$.

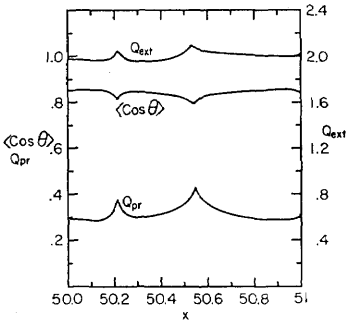

FIG. 4. Asymmetry factor $\langle\cos\theta\rangle$ and cross sections for extinction Q_{ext} and radiation pressure Q_{pr} for dielectric spheres with $m=1.33$. Computations made for $x=50(0.01)$ 51.

(2) $\langle cos\theta\rangle$. The major oscillations are much less apparent in $\langle\cos\theta\rangle$ than in Q_{ext}.

The minor oscillations, however, are obvious and are just out of phase with the ripple in Q_{ext}. Hence we have sharp resonance valleys rather than narrow peaks. Physically, this means that the extra energy removed from the beam in the resonance peaks of Q_{ext} is scattered more isotropically than the main component of the scattered energy, which tends to be concentrated in the forward direction.

Superimposed on the oscillations is a gradual rise in the values of $\langle\cos\theta\rangle$, as indicated by the values for $x\gg1$.[13]

(3) Q_{pr}. There is an initial peak in the cross section for radiation pressure, but there are no major oscillations.

Because the ripples in Q_{ext} and $\langle\cos\theta\rangle$ are out of phase, the minor oscillations are much more pronounced in Q_{pr} than in the other quantities. For example, for $m=1.50$ and $14.0<x<14.05$, Q_{pr} has a peak that is 50% higher than the value of x at the end points of this range. These resonance peaks become sharper as x increases and appear earlier for larger values of ν.

An interesting aspect of the ripple is illustrated clearly for the first time by the present computations. Notice, particularly for Q_{pr} and $\langle\cos\theta\rangle$ in Fig. 1 and for $\langle\cos\theta\rangle$ with $\tan\beta=0.01$ in Fig. 6a, that minor oscillations first appear for $x\leq2$, *are then damped out*, and then reappear at larger x. Moreover, the initial minor oscillations have a longer period than the "revived" oscillations (≈1.3 as contrasted to ≈0.9, for $m=1.20$). It

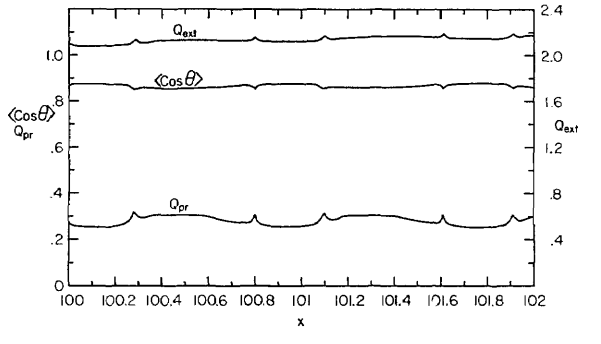

FIG. 5. Asymmetry factor $\langle\cos\theta\rangle$ and cross sections for extinction Q_{ext} and radiation pressure Q_{pr} for dielectric spheres with $m=1.33$. Computations made for $x=100(0.01)$ 102.

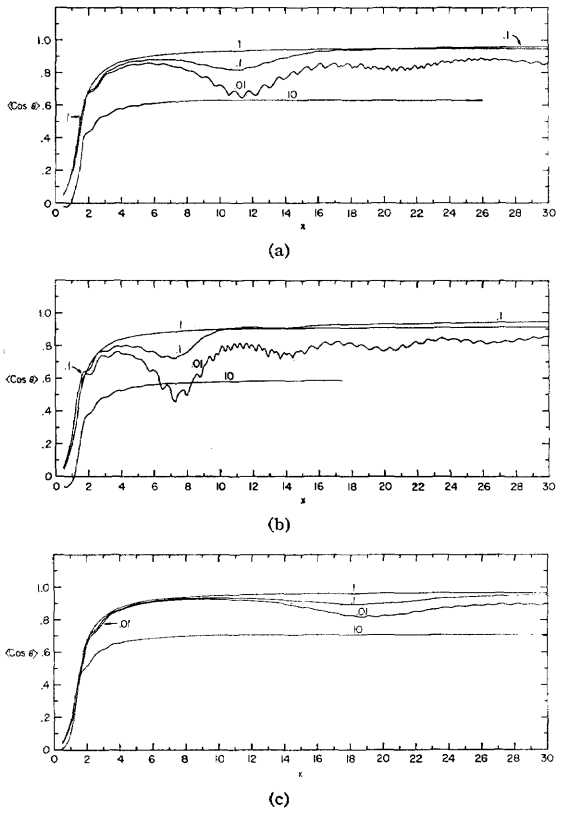

FIG. 6. Asymmetry factor $\langle\cos\theta\rangle$ for absorbing spheres. Curves are labeled with values of $\tan\beta=\nu'/(\nu-1)$, where $m=\nu-i\nu'$. (a) $\mathrm{Re}(m)=1.33$; (b) $\mathrm{Re}(m)=1.50$; (c) $\mathrm{Re}(m)=1.20$.

seems evident that a different effect is at work in the two cases. The initial oscillations can be explained as the result of standing waves excited in the scattering sphere (L. S., Sec. 10.5); i.e., they arise from interference between rays which suffer multiple internal reflections. The ripple which occurs at larger x must have another explanation, since the internally reflected rays would not have sufficient energy to produce the observed effect and would give rise to oscillations with a longer period [$\Delta x=\pi/(2m)=1.31$ for $m=1.20$, close to the observed value for the initial oscillations]. It seems likely that the "revived" minor oscillations are the result of surface waves. Probert-Jones[20] has used such an explanation to account for the ripple in the back-scattering cross section of ice spheres. More recently, Walstra[21] has examined the ripple phenomenon in detail on the basis of previously published values of Q_{sca} and has found excellent agreement with the tentative explanation given by van de Hulst (L. S., Sec. 17.52).

The approach to the asymptotic values appropriate

[20] J. R. Probert-Jones, *ICES Electromagnetic Scattering*, edited by M. Kerker (The Macmillan Company, New York, 1963), p. 237.

[21] P. Walstra, Proc. Kon. Ned. Akad. Wet. Amsterdam, Ser. B, **67** (in press).

for $x \gg 1$ is not rapid for dielectrics and is particularly slow for Q_{pr}. Even for $100 \leq x \leq 102$, Q_{pr} is still between 10% and 25% above the limiting value given by Irvine[13] for $m=1.33$. In contrast, Q_{ext} is between 4% and 6.5% high for x in this range, while $\langle\cos\theta\rangle$ is 1%–3% low.

Absorbing Spheres

Attenuation of the narrow peaks in the ripple structure begins to appear for $\tan\beta=0.001$. For $\tan\beta=0.01$, the very narrow peaks (width $\Delta x<0.1$) in Q_{pr} and Q_{ext} have been eliminated (Figs. 6 and 7) and the narrow valleys in $\langle\cos\theta\rangle$ have disappeared. The first component of the ripple (for those values of x for which the second component has not yet appeared) is strongly damped only for $\tan\beta=0.1$. By the time $\tan\beta=1$ the ripple has completely disappeared, as have the major oscillations. For $m \gtrsim 1.33$, the initial maximum in the radiation pressure, characteristic of perfectly reflecting spheres (L.S., Fig. 28), has begun to appear.

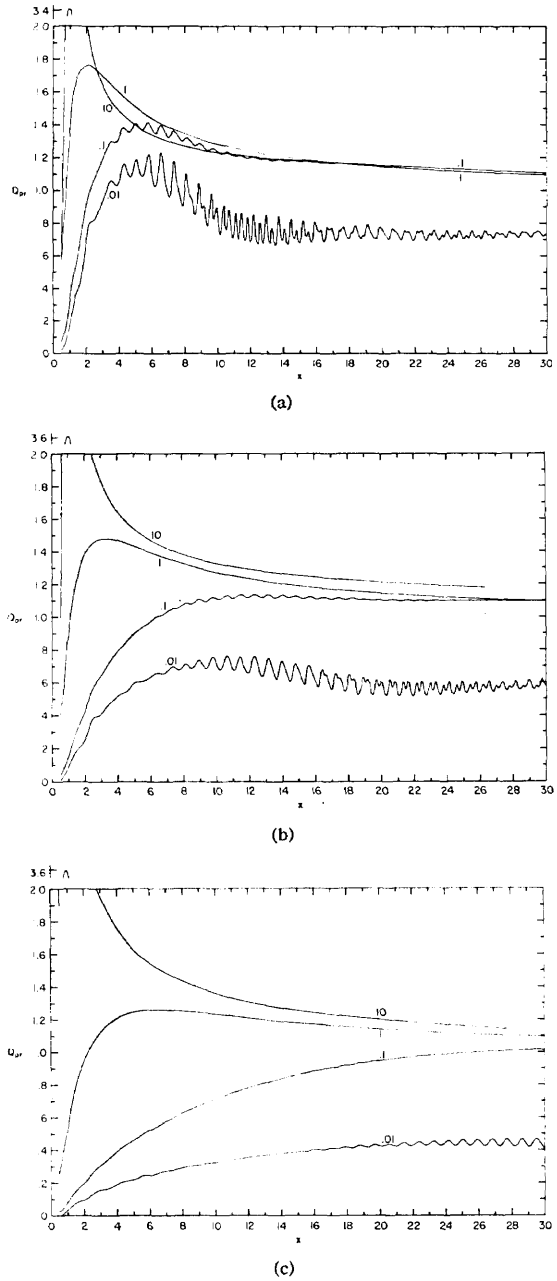

FIG. 7. Cross section for radiation pressure Q_{pr} for absorbing spheres. Curves are labeled with values of $\tan\beta=\nu'/(\nu-1)$, where $m=\nu-i\nu'$. Spot checks with $\Delta x=0.01$ show no further details. (a) $\mathrm{Re}(m)=1.50$; (b) $\mathrm{Re}(m)=1.33$; (c) $\mathrm{Re}(m)=1.20$.

As the absorption increases still further, minor oscillations reappear in Q_{ext} (Fig. 8), Q_{sca}, and (less obviously) in Q_{pr} and $\langle\cos\theta\rangle$. Although the ripple in the cross sections for infinite m is well known, this phenomenon does not seem to have been reported previously for spheres of large but finite conductivity. The peaks of the ripple appear at nearly the same x values for all m considered (contrary to the case for $\tan\beta<1$), the peaks being only slightly shifted toward smaller x for smaller $|m|$. It is interesting to note that the height of the first maximum in Q_{ext} is not a monotonic function of $\mathrm{Re}(m)$ or $|m|$, being larger for $m=1.33-3.3i$ than for $m=1.20-2i$ or $1.50-5i$ (Fig. 8). Because of the high conductivity of such particles, these minor oscillations must represent surface effects. This impression is strengthened by an examination of their period, which is nearly the same for all m considered ($\Delta x=0.75$ for $m=1.20$, increasing slightly with both x and $|m|$) and approximately the same as the period predicted by the theory of surface waves on perfect conductors (L. S., Sec. 17.41).

VERY LARGE SPHERES

The asymptotic value of Q_{ext} is 2 for any $m \neq 1$ for both dielectric and absorbing spheres.

As long as any absorption is present, the limiting value of $\langle\cos\theta\rangle$ is almost independent of $\tan\beta$ for $0<\tan\beta \lesssim 1$ for those values of m that we have considered. As $\tan\beta$ increases beyond 1, $\langle\cos\theta\rangle$ drops sharply (see Table I).

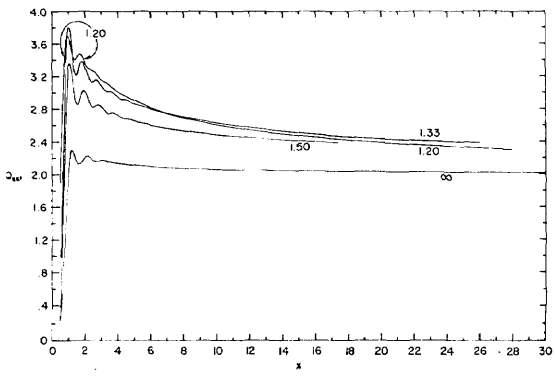

FIG. 8. Extinction cross section Q_{ext} for metallic spheres with $\tan\beta=10$ and $\mathrm{Re}(m)\equiv\nu$ as indicated.

The asymptotic value of Q_{pr} is also essentially constant for $0<\tan\beta\lesssim 1$, and shows only a slight increase for $1\lesssim\tan\beta\lesssim 10$.

The scattering cross section Q_{sca} behaves similarly to Q_{pr}, with a larger increase for $\tan\beta>1$.

It is also interesting to note the rate at which the various cross sections approach their asymptotic values as x increases for fixed ν. We might expect that the asymptotic values would be approached more rapidly for larger $\tan\beta$. This is indeed true for $0\lesssim\tan\beta\lesssim 1$, particularly for $\langle\cos\theta\rangle$. For example, with $m=1.33-0.33i$ and $x=30$, Q_{pr} exceeds $Q_{pr}(x\gg 1)$ by about 13%; Q_{ext} is about 8% high, while $\langle\cos\theta\rangle$ is within a few tenths of a percent of its limiting value (see Figs. 6–8 and Table I). For $\tan\beta$ in the range characteristic of conductors ($\tan\beta>1$), however, the approach to the asymptotic values occurs more slowly than for "absorbing dielectrics."

ACKNOWLEDGMENTS

I am grateful to Professor H. C. van de Hulst for reading a first draft of this paper and for several helpful suggestions, and to Dr. P. Walstra for providing me with a preprint of his paper. The programs used for the computations were written by James Francis and Jerome Cherniack, whose assistance is greatly appreciated.

JOURNAL OF THE OPTICAL SOCIETY OF AMERICA VOLUME 55, NUMBER 1 JANUARY 1965

Theory of Absorption and Scattering Within Integrating Spheres

P. J. RICHETTA

U. S. Army Biological Laboratories, Fort Detrick, Frederick, Maryland 21701

(Received 8 August 1963; Revision received 27 July 1964)

This paper reports a theory of integrating spheres filled completely with absorbing and scattering material. The development is oriented toward describing the behavior of such an integrating sphere when it is used as a spectrophotometer. The output ratio and effective light-path length of an integrating sphere spectrophotometer are introduced. Equations of radiative transfer theory are given for the determination of the output ratio and effective path length. Several approximations are derived for integrating sphere spectrophotometers having absorption but no scattering in the interior volume. Finally, the equations for an angularly symmetric spherical cavity having absorption and scattering are reduced to solution of the equations for a sphere having a perfectly absorbing wall.

1. INTRODUCTION

THE theory of the integrating sphere and the utility of this device for optical measurements are becoming familiar. As yet, however, there has been scant attention to the theory of diffuse-walled spheres filled completely with scattering and absorbing material. This paper reports an extension of the usual theory[1–4] to cover this case. Our main concern is to obtain a theoretical description of the "diffuse-light absorption vessel" (DLAV) of Bateman and Monk.[5]

In the DLAV, the absorbing sample completely fills an integrating sphere. Light is injected through a small opening in the sphere wall and flux output measurements are made at another small opening. When light in the interior of the DLAV reaches the wall, it is largely returned to the interior. This promotes interaction with absorbing components and masks scattering effects. Many methods have been used to do this in spectrophotometric work.[6–23] However, our experimental work with bacterial suspensions, erythrocytes, and polystyrene latex suggests that the DLAV is particularly effective in masking scattering effects.

This report begins with the definition of the DLAV output ratio, which is directly measurable. A derived quantity, the DLAV effective path length, is also intro-

---

[1] R. Ulbricht, *Das Kugelphotometer (Ulbricht'sche Kugel)* (Oldenbourg, Muenchen and Berlin, 1920).
[2] P. Moon, J. Opt. Soc. Am. **30**, 195 (1940).
[3] John A. Jacquez and Hans F. Kuppenheim, J. Opt. Soc. Am. **45**, 460 (1955).
[4] J. W. T. Walsh in *A Dictionary of Applied Physics*, edited by R. Glazebrook (Peter Smith, New York, 1950), Vol. IV, p. 435.
[5] J. B. Bateman and G. W. Monk, Science **121**, 441 (1955).
[6] O. Warburg and W. Christian, Biochem. Z. **266**, 377 (1933).
[7] D. L. Drabkin and R. B. Singer, J. Biol. Chem. **129**, 730 (1939).
[8] A. Dognon, Compt. Rend. Soc. Biol. **135**, 113 (1941).
[9] A. Dognon, Compt. Rend. Soc. Biol. **135**, 146 (1941).
[10] L. N. M. Duysens, thesis, Utrecht (1952).
[11] B. Chance, L. Smith, and L. Castor, Biochim. Biophys. Acta **12**, 289 (1953).
[12] R. Barer, J. Physiol. (London) **119**, 52 (1953).
[13] B. Chance, Science **120**, 767 (1954).
[14] L. N. M. Duysens, Science **120**, 353 (1954).
[15] K. Shibata, A. A. Benson, and M. Calvin, Biochim. Biophys. Acta **15**, 461 (1954).
[16] O. Warburg and G. Krippahl, Z. Naturforsch. **9b**, 181 (1954).
[17] R. Barer, Science **121**, 709 (1955).
[18] L. N. M. Duysens, Biochim. Biophys. Acta. **19**, 1 (1956).
[19] G. F. Lothian and P. C. Lewis, Nature (London) **178**, 1342 (1956).
[20] J. A. Bastin, E. W. J. Mitchell, and J. Whitehouse, Brit. J. Appl. Phys. **10**, 412 (1959).
[21] P. Latimer, Plant Physiol. **34**, 193 (1959).
[22] J. B. Thomas and Govindjee, Biophys. J. **1**, 63 (1960).
[23] Govindjee, Biophys. J. **1**, 373 (1961).